Research Paper

Earthquake-Induced Landslides Hazard Zonation of Sarpol-e Zahab Using Entropy Shannon Model

Vahid Tajik[1,5], Nasser Hafezi Moghaddas[2], Ebrahim Haghshenas[3], Hossein Sadeghi[4] and Masoumeh Rakhshandeh[5]*

1. Ph.D. Candidate, Engineering Geology, Ferdowsi University of Mashhad, Mashhad, Iran, *Corresponding Author; email: vtajik@gmail.com
2. Professor, Ferdowsi University of Mashhad, Mashhad, Iran
3. Associate Professor, Geotechnical Engineering Research Centre, International Institute of Earthquake Engineering and Seismology (IIEES), Tehran, Iran
4. Associate Professor, Ferdowsi University of Mashhad, Mashhad, Iran
5. Researcher, Geotechnical Engineering Research Centre, International Institute of Earthquake Engineering and Seismology (IIEES), Tehran, Iran

Received: 07/05/2023
Revised: 10/10/2023
Accepted: 30/10/2023

ABSTRACT

Earthquake of November 11, 2017 (Mw=7.3) in Ezgeleh village of Sarpol-e Zahab city in Iran, triggering numerous slope instabilities of various types of rockfalls, rockslides, avalanches and mud flows. The existence of a very high inherent potential and susceptibility of the region, on the one hand, and the occurrence of a strong earthquake as a driving factor, on the other hand, have been the main reasons for the instabilities in the region have been the main reasons for the instabilities in the region. The number of slope instabilities caused by this earthquake was rare compared to earthquakes with similar magnitude and thus requires more detailed investigations. The main objective of this study is to make a landslide hazard zonation map in this region, using Entropy Shannon's model, and compare the results with the landslides that triggered by the Ezgeleh earthquake. The landslide conditioning factors such as Slope Angle, Lithology (geology), Geological Strength Index (GSI), Slope Aspect, Distance to Faults, Pick Ground Acceleration (PGA), Plan Curvature, Distance to Roads, Distance to Rivers, Land Use, Normalized Difference Vegetation Index (NDVI) and Topographic Wetness Index (TWI), were extracted from the spatial database. By using these factors, weights of each factor were analyzed by index of Entropy model and the map of landslide hazard zonation were prepared, using Geographical Information System (GIS). The results showed that more than 31.37% of the surface of the area has a moderate to very high hazard of landslides. From 335 landslides identified, 235 (≈ 70%) locations were used for the landslide susceptibility maps, while the remaining 100 (≈ 30%) cases were used for model validation. Finally, the ROC (receiver operating characteristic) curve for landslide hazard zonation map was drawn and the areas under the curve (AUC) were calculated. The verification results showed that the index of Entropy model (AUC = 84.3%) has a high accuracy that is assumed as very good.

Keywords:
Landslide hazard zonation; Geographical Information System (GIS); Sarpol-e Zahab earthquake; Entropy shannon model; ROC curve

1. Introduction

Landslides are the downward and outward movement of a slope consisting of a rock, soil or artificial fill material under the influence of gravity, slope, water and other external forces and are one of the most important natural hazards (IAEG Commission on Landslides, 1990). Landslides and slope instabilities are one of the most widespread and destructive natural hazards in highlands and

mountainous regions. In special conditions, landslides can be a serious natural hazard worldwide that cause high numbers of fatalities and damage to properties every year (Froude & Petley, 2018). They can be triggered by other hazards such as earthquakes (Lee & Evangelista, 2006; Karakas, et al., 2021a) and heavy rainfalls (Dikshit et al., 2020; Kocaman et al., 2020), as well as by anthropogenic activities (Sevgen et al., 2019; Yanar et al., 2020). The impact of landslides can be far-reaching, including loss of lives and properties, damage to infrastructures such as water supply, electricity, gas line, transportation, sewage system, as well as to landscape and environment.

By investigating the occurred landslides, we gain knowledge about the spatial occurrence of landslides and improve our understanding of the underlying processes causing landslides (Yanar et al., 2020). The study of landslides reaches from site-specific field investigations to global datasets of landslides and from event based inspections to long-term monitoring for several years (Alberti, et al., 2020; Coe, 2020; Mateos et al., 2020; Svennevig et al., 2020a). Among the different spatial and temporal approaches of landslide studies, landslide inventory mapping is a common method to investigate the spatial occurrence of landslides (Guzzetti et al., 2012; Galli et al., 2008; Hao et al., 2020).

The study of landslides has drawn global attention mainly to the increasing awareness of their socio-economic impacts as well as the increasing pressure of urbanization on the mountain en-vironments (Aleotti & Chowdhury, 1999). Statistics from the Center for Research on the Epidemiology of Disasters (CRED) show that landslides are responsible for at least 17% of all fatalities from natural hazards worldwide. This trend is expected to continue in the future due to the increase of the unplanned urbanization and development, deforestation, and regional precipitation as a result of changing climatic conditions in landslide-prone areas (Goetz et al., 2011; Kanungo, 2006; Schuster, 1996). Landslides cause loss of life and property, and damage to natural resources, developmental projects, and essential commodities. The mountainous areas of Iran are prone to landslides, causing a lot of damage every year, especially after a moderate to high magnitude earthquakes. As an instance, during the Manjil earthquake in 1990, Ms 7.3, 187 people died merely by triggered landslides (ILWP, 2007). Losses resulting from mass movements until the end of September 2007 have been estimated at 126,893 billion Iranian Rials using the 4900 landslide database (ILWP, 2007). Considering the importance of recognizing, the occurrence risk factors in landslide hazards zoning is necessary (ILWP, 2007). Mountainous features, high tectonic activity, and geological and climatological variety make the Iranian plateau capable of the occurrence of various types of landslides (especially in the Alborz and Zagros active mountainous belts). One of the ways to reduce landslide damage is landslide hazard zonation mapping. The aim of the zonation methods is to identify areas that are susceptible to future landslides, based on the knowledge of past landslide events and terrain parameters, geological attributes, and other possibly anthropogenic environmental conditions that are associated with the presence or absence of such phenomena. During recent decades, the use of landslide susceptibility and hazard maps for land use planning has increased significantly. These maps rank different sections of the land surface according to the degree of actual or potential landslide hazard; thus, planners are able to choose favorable sites for urban and rural development (Pourghasemi et al., 2012).

2. Data, Materials and Method

2.1. Study Area

The study area is the affected region by the November 11, 2017 earthquake (Mw = 7.3) in Ezgeleh village of Sarpol-e Zahab, west of Kermanshah province (Figure 1). The area is about 3774 km^2 lies between the longitudes 45°41' to 46°16' E, and latitudes 34°4' to 34°54' N. Altitude in the study area varies between 371 and 2559 m a.s.l. The region is covered by various types of lithological formations including Paleozoic (Permian), Mesozoic and Cenozoic. Most of the slope instabilities occurred in the Rijab syncline, Shah-Neshin Mountain and Dalahoo Heights, which consists of limestone of the Asmari formation (Oligo-Miocene) and Pabdeh formation (shale,

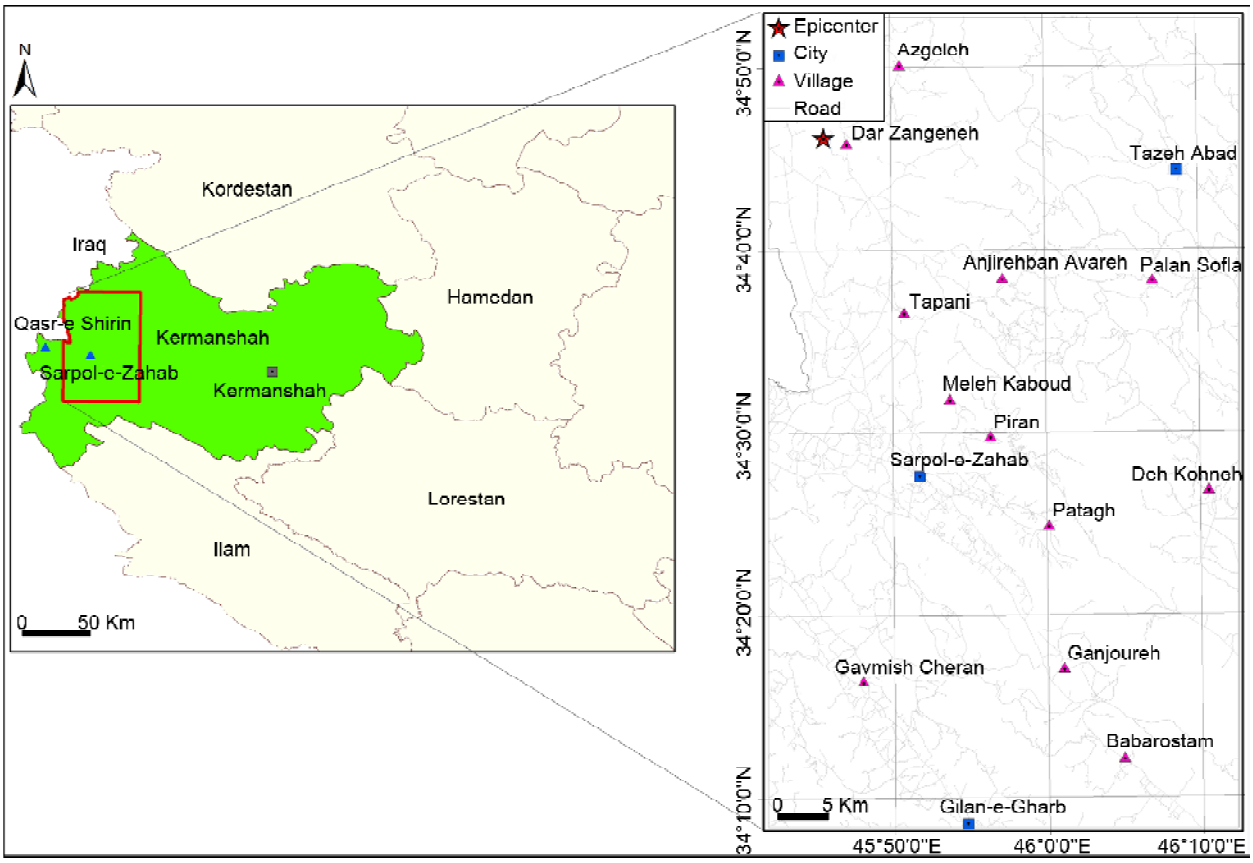

Figure 1. Map of the study area (is located in the area affected by the November 11, 2017 earthquake in Sarpol-e Zahab).

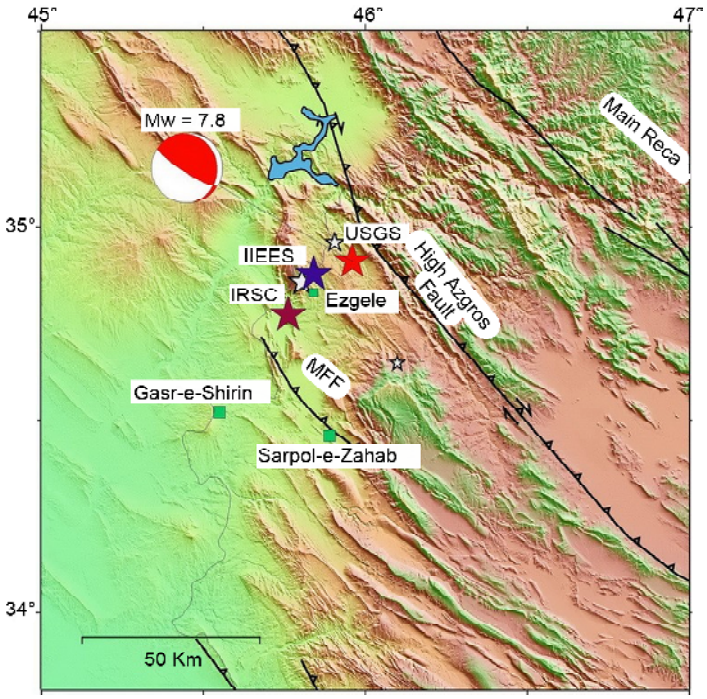

Figure 2. Location of Sarpol-e Zahab earthquake's epicenter (November 11, 2017) (IIEES, 2017).

limestone and clay). The difference in the hard layers of the Asmari formation on the soft layers Pabdeh formation along with the tectonic structures has caused the area to be prone to the instability (IIEES, 2017) (Figure 2).

2.2. Datasets

2.2.1. Landslides Inventory Map

One clue to the location of future landslides is the distribution of past movements; hence maps

that show the location and size of landslides (landslide inventory maps) are helpful in predicting the hazard for an area. The landslide inventory map of the study area was identified and manually delineated by experts through visual interpretation of air photos, satellite images (Google Earth) and field observations. 335 landslide polygons with the total coverage area about 20.4 km^2 are identified. The landslide inventory map of the study area is presented in Figure (3). The spatial distribution of slope instabilities is caused by earthquake in a wide area of the region, so that it covers from the north of Sarpol-e Zahab to near Ilam (in the southeast). Such a wide dispersion of these phenomena has been observed less compared to other earthquakes of similar magnitude (IIEES, 2017).

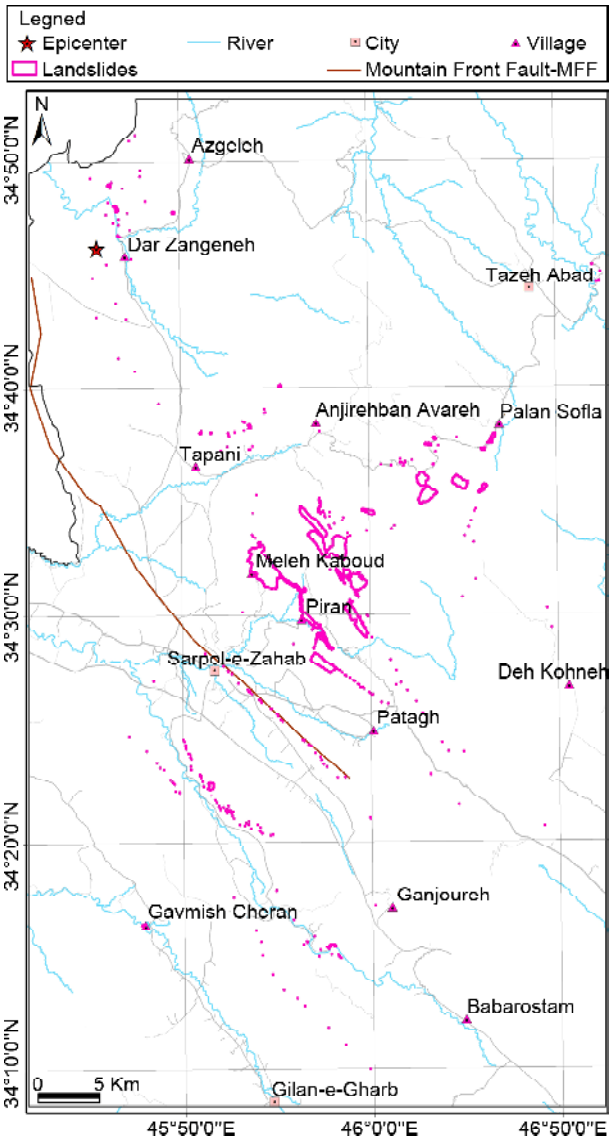

Figure 3. Landslides inventory map of the study area.

Satellite images and field observations showed that most of slope instabilities are concentrated in the Rijab syncline, Shah-Neshin Mountain and Dalahoo Heights. These various types of slope instability such as rockfalls, avalanches, soil slides, rockslides and mud flow have occurred in study area, but rock and soil slides are more abundant. The largest landslide is "Mella Kabud-Qorchi Bashi", the dimensions of which are about 4×4 km (Figure 3).

The number of induced earthquake landslides of this earthquake has been unprecedented in recent decades in Iran. Some other types of landslides caused by the Sarpol-e Zahab earthquake are rockfall zones in Baba Yadegar valley, rock avalanche zones waterfall, the landslide of north Dalahoo, and the Rock slide of Chenareh, which are explained below in details (IIEES, 2017).

2.2.1.1. The Mella Kabud-Qorchi Bashi Landslide

It is the biggest earthquake-induced landslide occurred in the study area with dimensions of approximately 4×4 km. This landslide is located a few kilometers north of Sarpol-e Zahab, and it is easily visible from a faraway distance. Many wide transverse cracks displaced mass of the main body, some of which are more than 1 km long and more than 40 m deep. The height of the main scarp reaches 15 m in some parts (IIEES, 2017). Figure (4), shows some images of this landslide (Figure 4).

2.2.1.2. The Baba Yadegar Valley Rockfall Zones

One of the most important rockfall zones caused by this earthquake is Baba Yadegar valley, located in the interior western part of the Rajab syncline. Dimensions of these rockfalls are up to six m^3 and the weight of more than 10 tons (Figure 5).

2.2.2. Landslide Effective Factors

To study the landslide hazard zonation, the researcher must be able to recognize the real causal factors that might lead to instability in a given area. Therefore, this is key information, since it helps in achieving accurate findings upon completion (Guzzetti et al., 2000). To make a

Figure 4. Images of the main scarp of the Mella Kabud-Qhorchi Bashi landslide and transverse cracks formed on the landslide-displaced mass of the main body.

Figure 5. Images of Baba Yadegar rockfall zones.

landslide hazard zonation map, it is necessary to select the parameters that have the greatest effect on the landslide event (Tajik, 2009; Rakhshandeh, 2018). In this way, according to the numerous field observations made in the region and using the expert and engineering by judgment method, 12 effective factors were identified and the desired layers were prepared. The effective factors were weighted between 0 (least effect) and 2 (greatest effect) based on their impact on the occurrence of landslides by judgment expert method (Table 1).

To make this map, first, the Digital Elevation Model (DEM) of the region was prepared by using topographic digital data by grid size of 4,205,215 pixels. Then the slope angle and slope aspect maps were extracted from the DEM of the area by ArcGIS. The slope angle map was categorized into seven classes (<5°, 5-10°, 10-15°, 15-25°, 25-35°, 35-45° & >45°), and slope aspect map into nine classes (Flat, North, North-East, East, South-East, South, South-West, West & North-West) (Figures 6 and 7). The geological map of the study area was obtained from four geological maps of Sarpol-e Zahab, Qasr-e Shirin, Bayangan and Kerend (1:100,000-scale), (Figure 8 and Table 1). The Geological Strength Index (GSI) map is prepared during the field studies (Figure 9 and Table 1). Based on the lithological and GSI maps, and using the RockLab software (Rocscience Inc., 2007), the values of φ' (cohesion) and c' (friction angle) of the rock masses was estimated and categorized into seven classes (Type-1 until 6). Also, using a geological map, the effective factor of Distances to faults map was calculated and categorized into five classes (0-25 m, 25-50 m, 50-75 m, 75-100 m and >100 m), (Figure 10 and

Table 1. The spatial relationship between each effective factor and landslides Hazard Zonation using the index of entropy model.

Parameter	Group	Class	*W* (Judgment Expert)	*Wf* (Entropy Shannon)
Slope Angle	1	<5	0.000	0.000
	2	10-May	0.100	0.010
	3	15-Oct	0.500	0.070
	4	15-25	1.000	0.140
	5	25-35	1.700	0.230
	6	35-45	1.950	0.260
	7	>45	2.000	0.270
PGA	1	< 200	0.400	0.010
	2	200-300	1.000	0.025
	3	300-400	1.400	0.035
	4	400-500	1.800	0.045
	5	> 500	2.000	0.050
Slope Aspect	1	Flat	0.000	0.000
	2	N	0.190	0.013
	3	NE	0.280	0.020
	4	E	0.030	0.002
	5	SE	0.090	0.006
	6	S	0.550	0.039
	7	SW	1.000	0.070
	8	W	0.750	0.053
	9	NW	0.320	0.022
Plan Curvature	1	Straight	0.300	0.012
	2	Concave	0.600	0.024
	3	Convex	1.000	0.040
Distance to Roads	1	> 60	0.000	0.000
	2	40 - 60	0.300	0.012
	3	20 - 40	0.600	0.024
	4	0 - 20	1.000	0.040
GSI	1	Landslide	2.000	0.220
	2	Soil Slopes, Very Soft and Loose Rocks	2-1.95	0.215
	3	Loose Stones	1.95-1.7	0.187
	4	Relatively Hard Stones	1.7-1	0.110
	5	Hard Stones	1-0.4	0.044
	6	Very Hard Stones	0.4-0	0.022
	7	Flat Quaternary Loose Sediments	0.000	0.000

Parameter	Group	Class	*W* (Judgment Expert)	*Wf* (Entropy Shannon)
Land Use	1	Rainy Land	0.100	0.000
	2	Dense Forest Lands	0.000	0.000
	3	Semi-Dense Forest Lands	1.000	0.010
	4	Lands of Sparse Forests	0.300	0.010
	5	Semi-Dense Pasture Lands	0.600	0.010
	6	Non-Dense Pasture Lands	0.300	0.000
	7	Cropland	0.000	0.000
	8	Built-Up	0.000	0.000
Distance to fault	1	> 100	0.000	0.000
	2	75 - 100	0.100	0.005
	3	50 - 75	0.300	0.015
	4	25 - 50	0.600	0.030
	5	0 - 25	1.000	0.050
Lithology	1	Type-1	0.000	0.000
	2	Type-2	0.200	0.022
	3	Type-3	0.600	0.066
	4	Type-4	0.700	0.077
	5	Type-5	0.900	0.099
	6	Type-6	1.100	0.121
	7	Type-7	1.500	0.165
	8	Type-8	1.700	0.187
	9	Type-9	2.000	0.220
Distance to Rivers	1	> 60	0.000	0.000
	2	40 - 60	0.300	0.006
	3	20 - 40	0.600	0.012
	4	0 - 20	1.000	0.020
NDVI	1	Water	0.000	0.000
	2	Rock/ Bare Soil	0.400	0.004
	3	Plant with Thin Cover	1.000	0.010
	4	Shrub	0.600	0.006
	5	Grassland	0.250	0.003
TWI	1	> 8	0.000	0.000
	2	10-Aug	0.000	0.000
	3	12-Oct	0.100	0.001
	4	14-Dec	0.300	0.003
	5	> 14	1.000	0.010

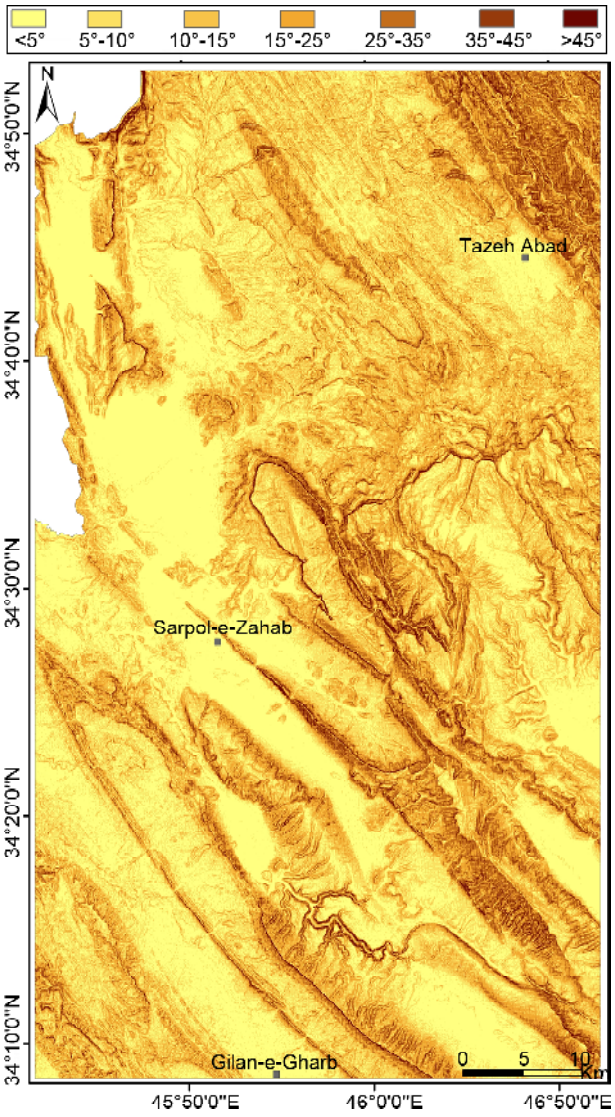

Figure 6. Effective Factor Maps; The Slope Angle map was categorized into seven classes (<5°, 5-10°, 10-15°, 15-25°, 25-35°, 35-45° and >45°).

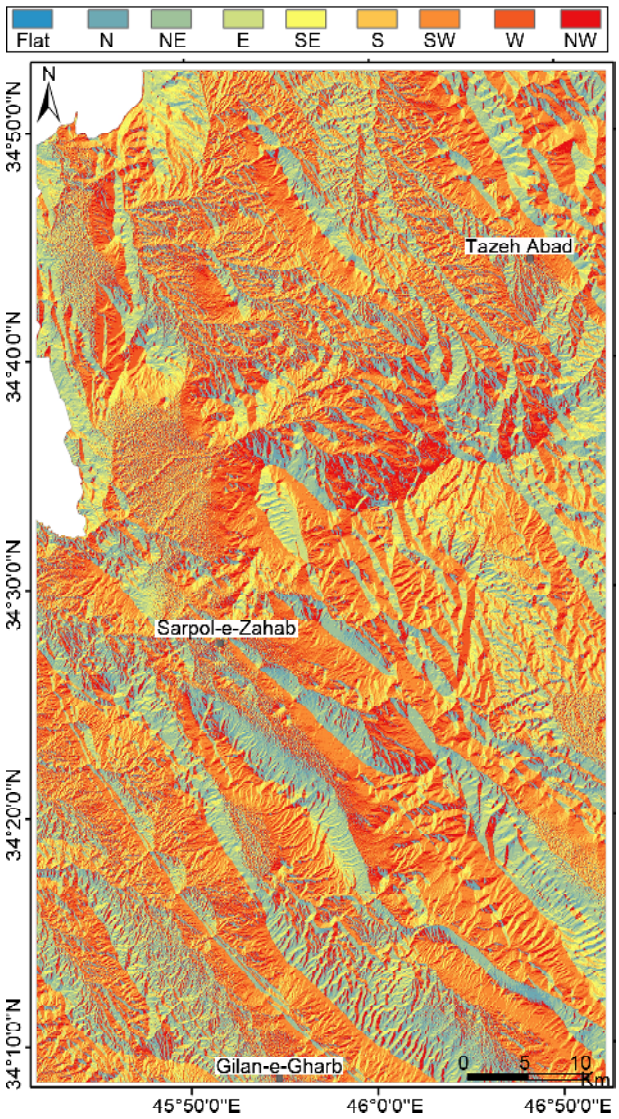

Figure 7. Effective Factor Maps; The Slope Aspect map was categorized into nine classes (Flat, North, North-East, East, South-East, South, South-West, West and North-West).

Table 1). The Peak Ground Acceleration (PGA) zoning map for return period of 2475 year (IIEES, 2017) was used for preparing the earthquake factor map. This map is categorized into five classes of 0-0.2 g, 0.2-0.3 g, 0.3-0.4 g, 0.4-0.5 g & > 0.5 g (Figure 11 and Table 1). In the case of the curvature, negative curvatures represent concave, zero curvature represents straight, and positive curvatures represent the convex surface. The plan curvature map was prepared in GIS and categorized into three classes (Straight, Concave & Convex), (Figure 12 and Table 1). In addition, the distance to roads and rivers was calculated using the topographic database. The maps of distance to roads and rivers categorized into four classes (0-20 m, 20-40 m, 40-60 m and >60 m) as shown in Figures (13) and (14) and Table (1). The Land Use map was categorized into eight classes (rainy land, dense forest lands, semi-dense forest lands, lands of sparse forests, semi-dense pasture lands, non-dense pasture lands, cropland and built-up) as shown in Figure (15) and Table (1). The Normalized Difference Vegetation Index (NDVI) was created using Landsat 8 satellite images of 2017. The final NDVI map shows values between -1.0 and +1.0, and then it was categorized into five classes (water/snow, rock/bare soil, plant with thin cover, shrub and grassland) (Figure 16 and Table 1). Among other parameters affecting the occurrence of landslides in the studied area is the Topographic Wetness Index (TWI). Topographical changes directly affect the hydrological

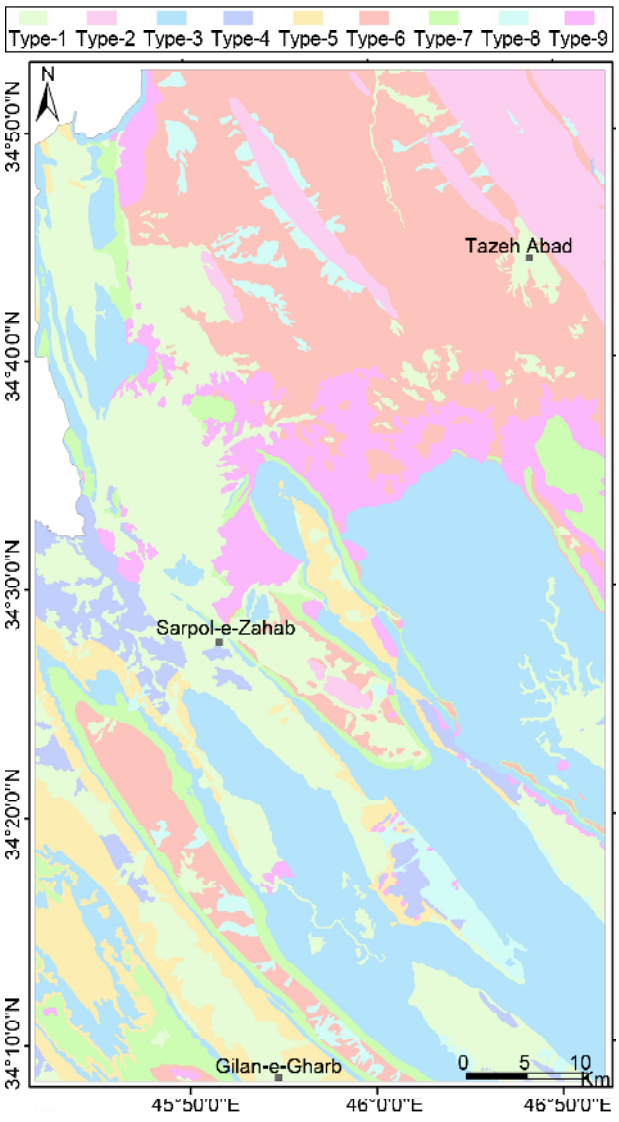

Figure 8. Effective Factor Maps; Lithological map extracted from geological map of the study area categorized into nine classes (Type-1 to 9).

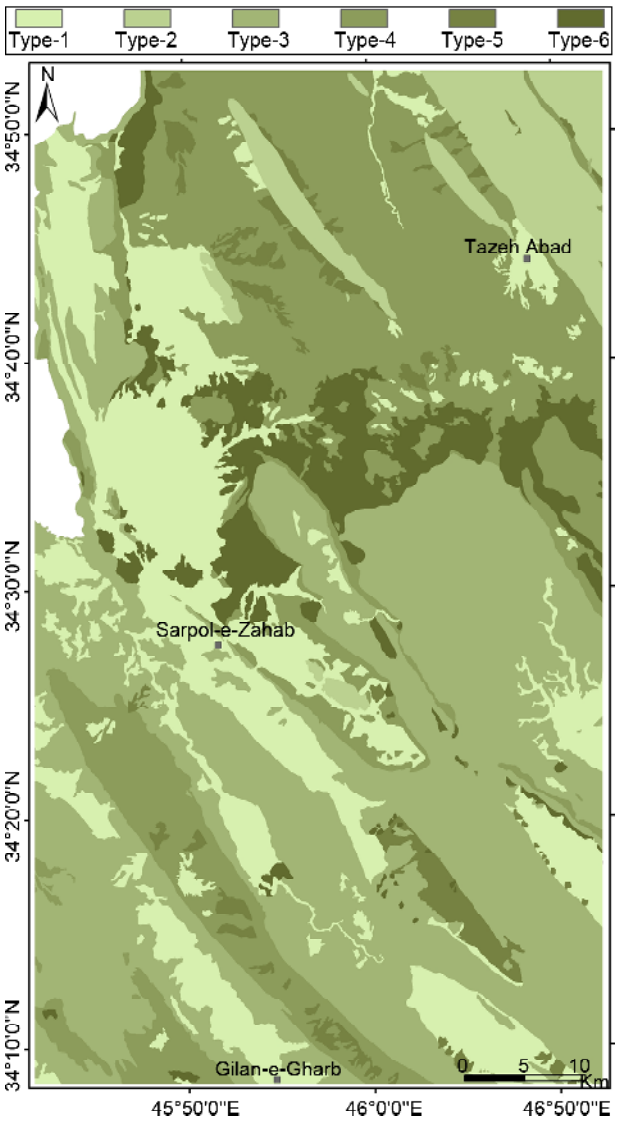

Figure 9. Effective factor maps; The geological strength index (GSI) categorized into seven classes (Type-1 to 6).

conditions and consequently the soil moisture level and the underground water level (Zinko et al., 2005; Sorensen et al., 2006). TWI map was categorized into five classes (<8, 8-10, 10-12, 12-14 & >14) as shown in Figure (17) and Table (1).

2.2.3. Methodology and Modeling

Figure (18) shows the different stages of the research method and preparing the landslide hazard zonation map. As mentioned in the sections 2.2.1 and 2.2.2, the first step in making landslide susceptibility maps is to prepare a distribution map of landslides occurred in the past. This stage is considered as the most important part and pre-requisite for susceptibility studies and landslide risk (Regmi, et al., 2014). For this purpose, first, the location of the landslides occurred in the region was identified using Google Earth images and extensive field visits, and a total of 335 landslides were detected in the region. In Table (1), the effective factors used in earthquake-induced landslides hazard zonation, as well as the subgroups of each of the input factors, are presented. As shown in Table (1), 12 factors were identified and investigated. For the current study, 12 landslides related effective factors were selected: Slope Angle, Lithology (geology), Geological Strength Index (GSI), Slope Aspect, Distance to Faults, Pick Ground Acceleration (PGA), Plan Curvature, Distance to Roads, Distance to Rivers, Land Use, Normalized Difference Vegetation Index (NDVI) and Topographic Wetness Index (TWI).

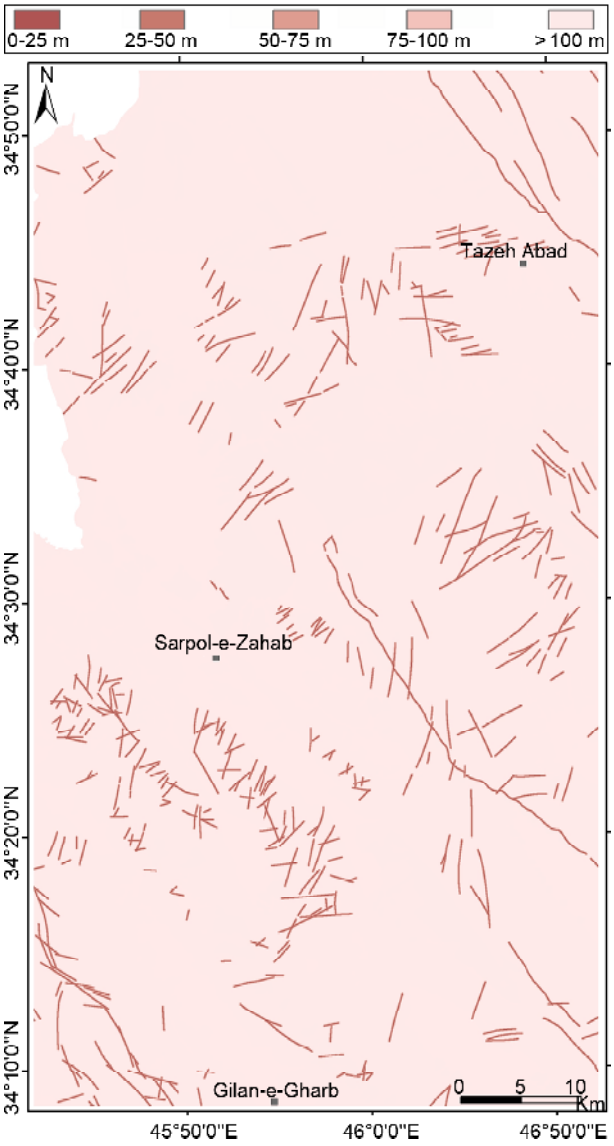

Figure 10. Effective Factor Maps; Distance to Faults map was calculated and categorized into five classes (0-25 m, 25-50 m, 50-75 m, 75-100 m and >100 m).

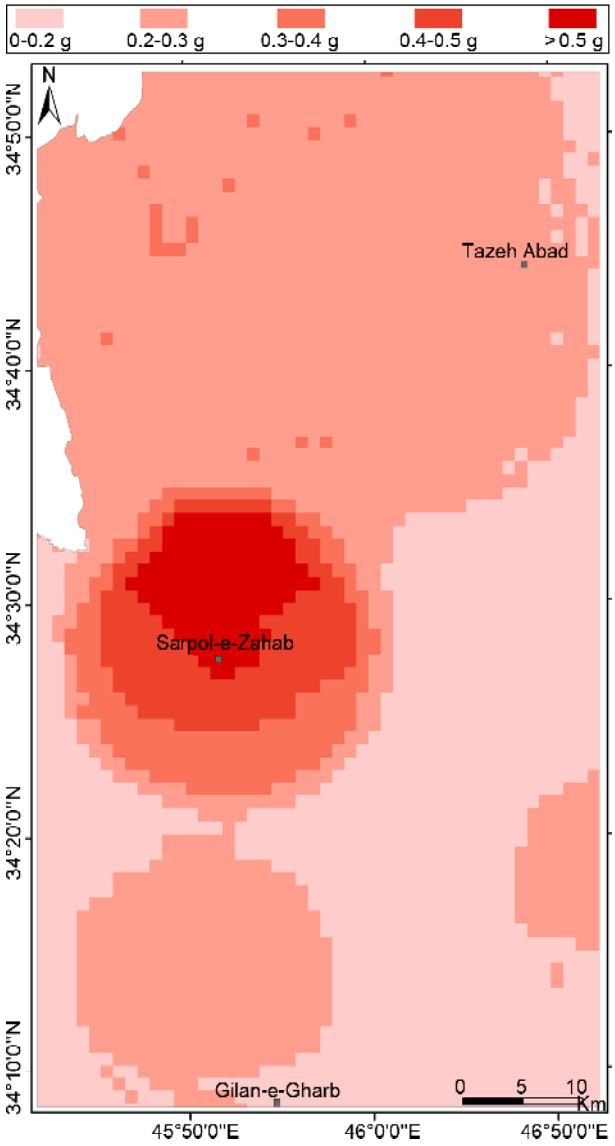

Figure 11. Effective Factor Maps; The PGA map was categorized into five classes of 0-0.2 g, 0.2-0.3 g, 0.3-0.4 g, 0.4-0.5 g and >0.5 g.

Shannon's entropy model was used to weight the effective factors in the occurrence of landslides in the study area. Shannon entropy is a model for measuring a disordered, instability, imbalance and uncertainty of a system. The quantity of entropy of a system has a one-to-one relationship with the degree of disorder; this relationship, called the Boltzmann principle, has been used to describe the thermodynamic status of a system (Yufeng & Fengxiang, 2009). The principle of Boltzmann was expanded upon by Shannon, who established an entropy model for information theory. This way, the information entropy method has been widely used to determine the weight index of natural hazards and has been used for integrated environmental assessments of natural processes, such as sand storms, droughts, mud and debris flows (Li et al., 2002). Types of landslides are complex systems for the exchange of materials and energy with the environment, and thus a landslide can be measured and described using the information entropy method (Yang & Qiao, 2009). The entropy of a landslide refers to the extent that various factors influence the development of a landslide. Several important factors provide additional entropy into the index system. As a result, the entropy value can be used to calculate the objective weights of the index system (Yang et al., 2010). The weight value of each factor is expressed separately as the entropy

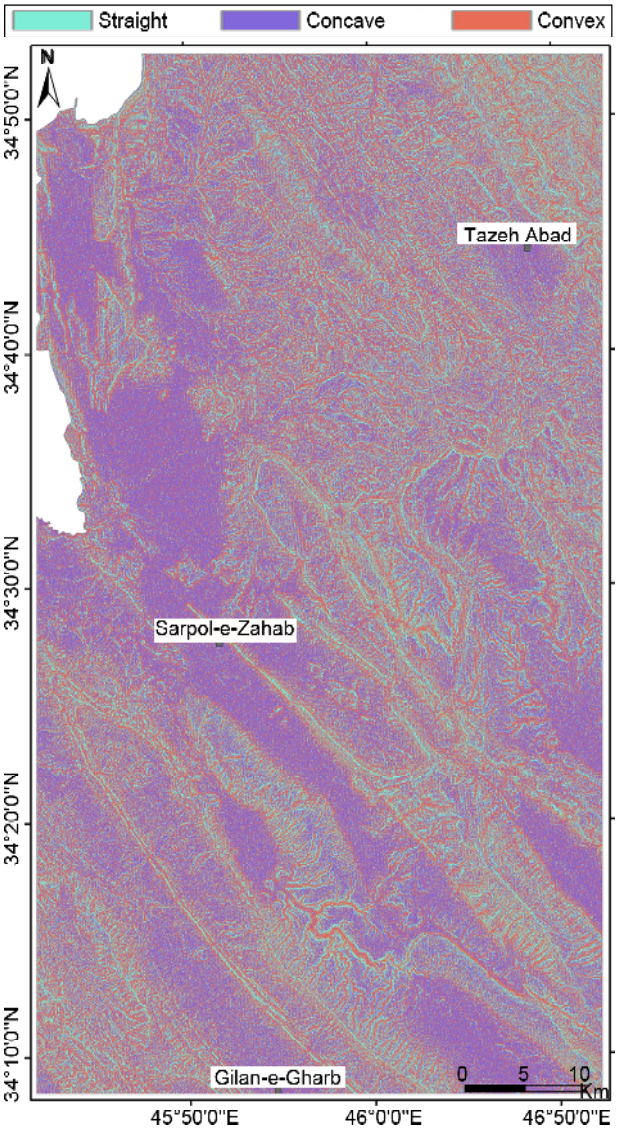

Figure 12. Effective Factor Maps; The Plan Curvature map was categorized into three classes (Straight, Concave and Convex).

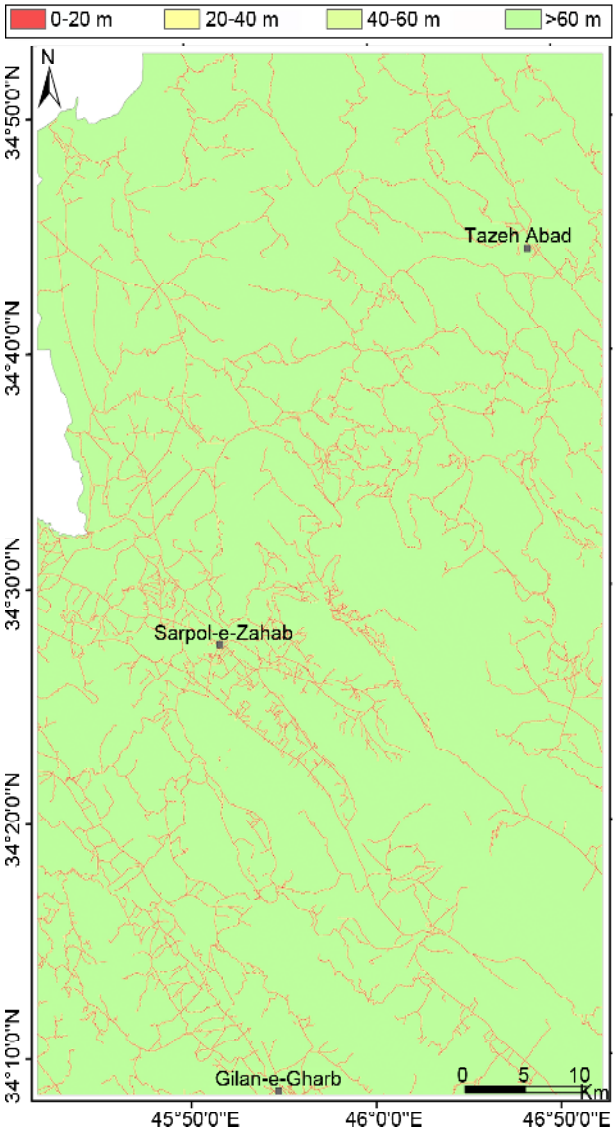

Figure 13. Effective Factor Maps; The Distance to roads map was categorized into four classes (0-20 m, 20-40 m, 40-60 m & >60 m).

index; as a result, by using this index, it is possible to identify the factors that have the greatest impact on the occurrence of landslides or any other phenomenon. In order to determine the weight related to each of the effective factors, Equations 1 to 5 were used (Bednarik et al., 2010; Pourghasemi et al., 2012; Devkota et al., 2013; Wang et al., 2016).

$$FR = \frac{A_l}{A_{cl}} \tag{1}$$

$$P_d = \frac{FR}{\sum_{C=1}^{Nc} FR} \tag{2}$$

$$En_{max} = \log_2 N_c \ , N_c - \text{number of classes} \tag{3}$$

$$I_c = \frac{En_{max} - En}{En_{max}} \quad c = 1, \ \ldots n \tag{4}$$

$$W_f = I_c * FR \tag{5}$$

where A_l is number of landslide pixels (%); A_{cl} is area of hazard zone category(%); FR is Frequency Ratio (%); P_d is the probability density; N_c is decision matrix; E_{nv} and E_{nv} max represent entropy values; I_c is the information coefficient and W_f is final weight of each factor.

3. Making and Verification of the Landslide Hazard Zonation Maps

Based on the results of examining the importance of each of the effective factors in the landslide

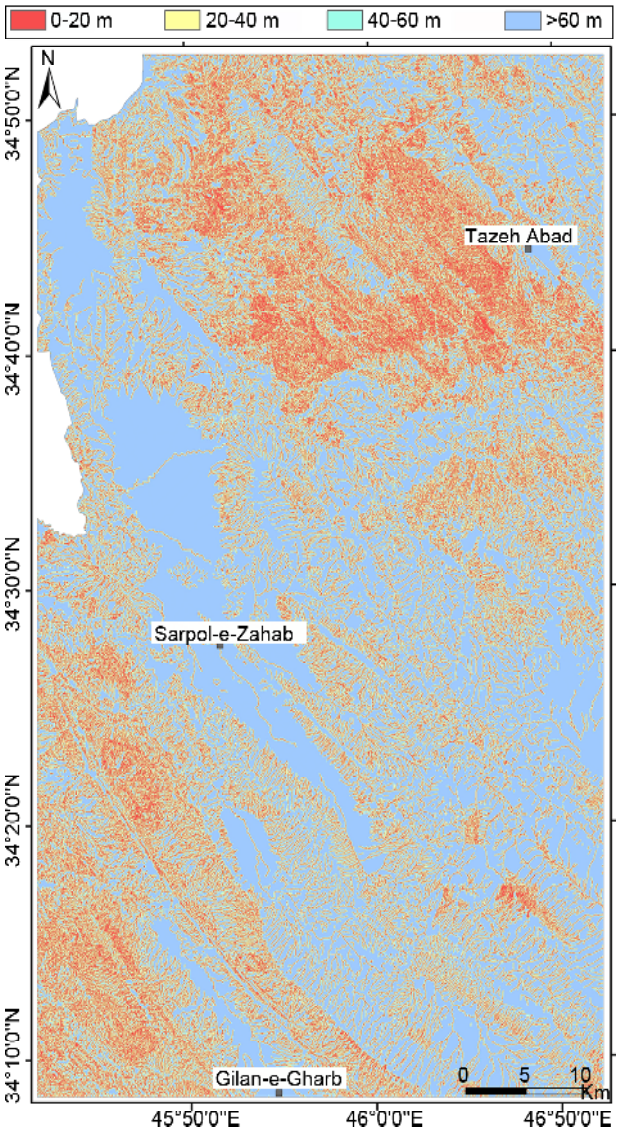

Figure 14. Effective Factor Maps; The Distance to rivers map was categorized into four classes (0-20 m, 20-40 m, 40-60 m & >60 m).

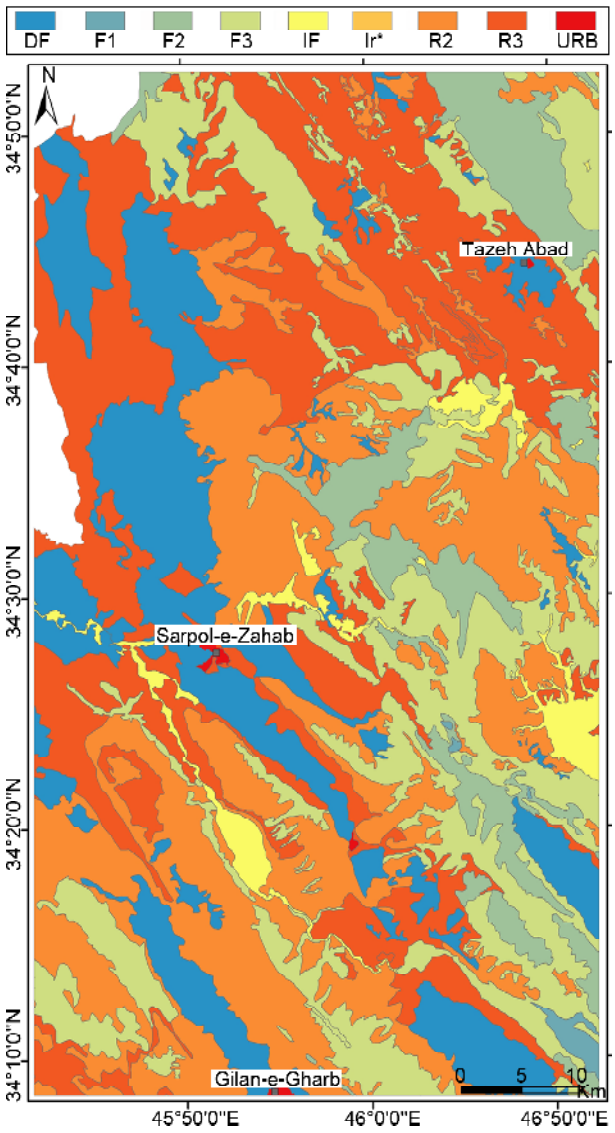

Figure 15. Effective Factor Maps; The Land Use map was categorized into eight classes (rainy land, dense forest lands, semi-dense forest lands, lands of sparse forests, semi-dense pasture lands, non-dense pasture lands, cropland and built-up).

event using Shannon's entropy index, it was determined that the layers of the Slope Angle, Lithology, Geological Strength Index (GSI), Slope Aspect, Distance to Fault, Pick Ground Acceleration (PGA), Plan Curvature, Distance to Roads, Distance to Rivers, Land Use, Normalized Difference Vegetation Index (NDVI) and Topographic Wetness Index (TWI) with 0.27, 0.22, 0.22, 0.07, 0.05, 0.05, 0.04, 0.04, 0.02, 0.01, 0.01, and 0.01 are from the highest to the lowest weight.

Finally, using the results of the entropy method, the effective factors were weighted as shown in Table (1). The final landslide hazard zonation map was prepared by the summation of weighted products of the effective parametric maps (Figure 19). After examining the importance of factors affecting the occurrence of landslides, the landslide hazard zoning map was prepared based on the relationships of the entropy model and divided into five classes that is Very Low, Low, Medium, High and Very High. The area corresponding to each of the classes is 45.23, 23.40, 11.42, 8.27 and 11.67 percent respectively (Figure 19). The area corresponding to each of the hazard classes was calculated as 11.67%, 8.27%, 11.42%, 23.40% and 45.23%, respectively. Also, the ratio of the areas involved in landslides to the hazard classes, from 68.94% (very high), 11.10% (high), 8.72% (medium), 9.65% (low) and

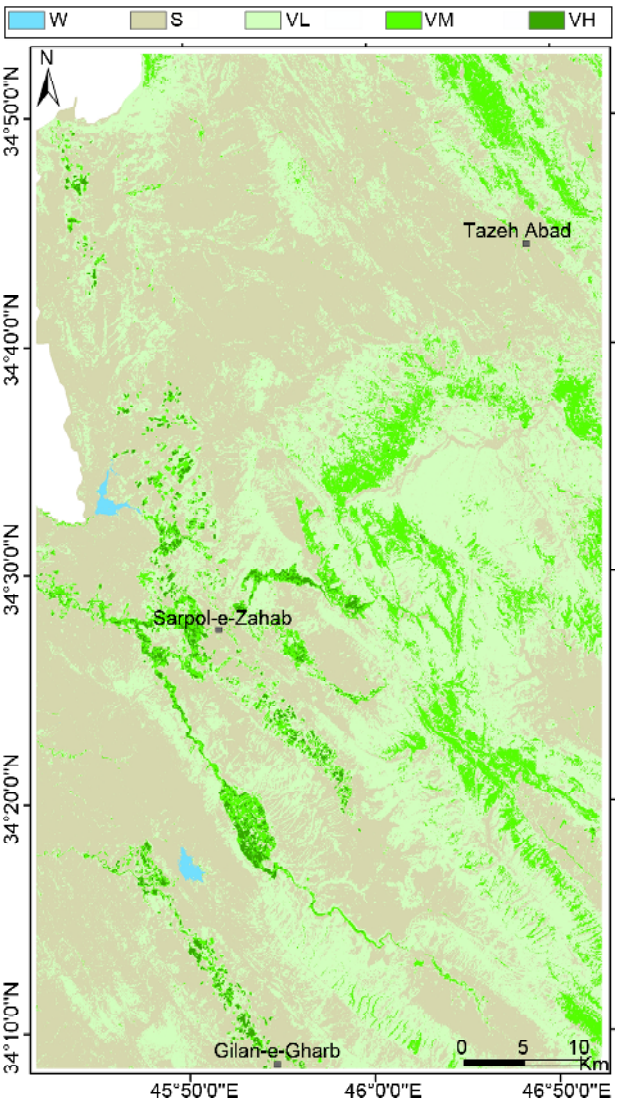

Figure 16. Effective Factor Maps; The NDVI map was categorized into five classes (water/snow, rock/bare soil, plant with thin cover, shrub and grassland).

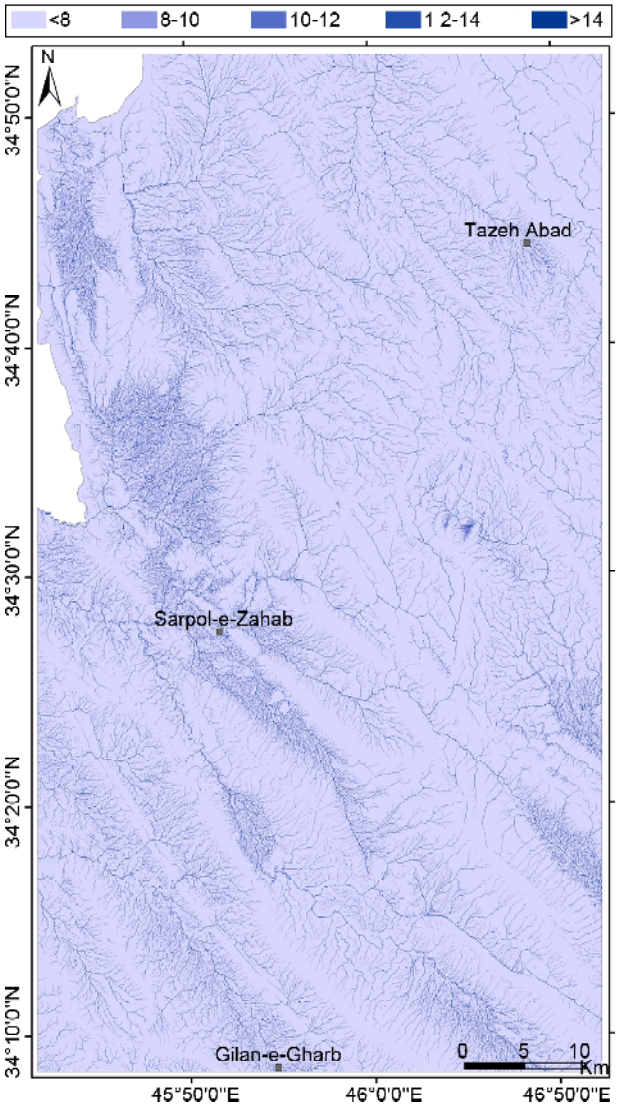

Figure 17. Effective Factor Maps; The TWI map was categorized into five classes (<8, 8-10, 10-12, 12-14 and >14).

Table 2. The area corresponding to each of the hazard classes in the region.

Classes	Total Landslide Area (m^2)		Landslide Area in Each Classes (m^2)	
Very Low	1705006327.41	% 45.23	323659.5598	% 1.59
Low	882181352.14	% 23.40	1967049.377	% 9.65
Medium	430663694.00	% 11.42	1776944.746	% 8.72
High	311692455.18	% 8.27	2263443.634	% 11.10
Very High	440032948.93	% 11.67	14053050.1	% 68.94
Sum	3769576777.66	% 100.00	20384147.41	% 100.00

59.1% (very low), it was estimated that finally, the total areas involved in landslides occurred in the very high and high category, with more than 80% showing the high accuracy of the landslide hazard zonation map (Figure 19). The area corresponding to each of the hazard classes in the region was calculated as 11.67%, 8.27%, 11.42%, 23.40% and 45.23%, respectively (Figure 20 and Table 2).

From 335 landslides identified, 235 ($\approx$70%) locations were used for the landslide susceptibility maps, while the remaining 100 ($\approx$30%) cases were used for model validation. Finally, the ROC (receiver operating characteristic) curve for the landslide hazard zonation map was drawn and the areas under the curve (AUC) were calculated.

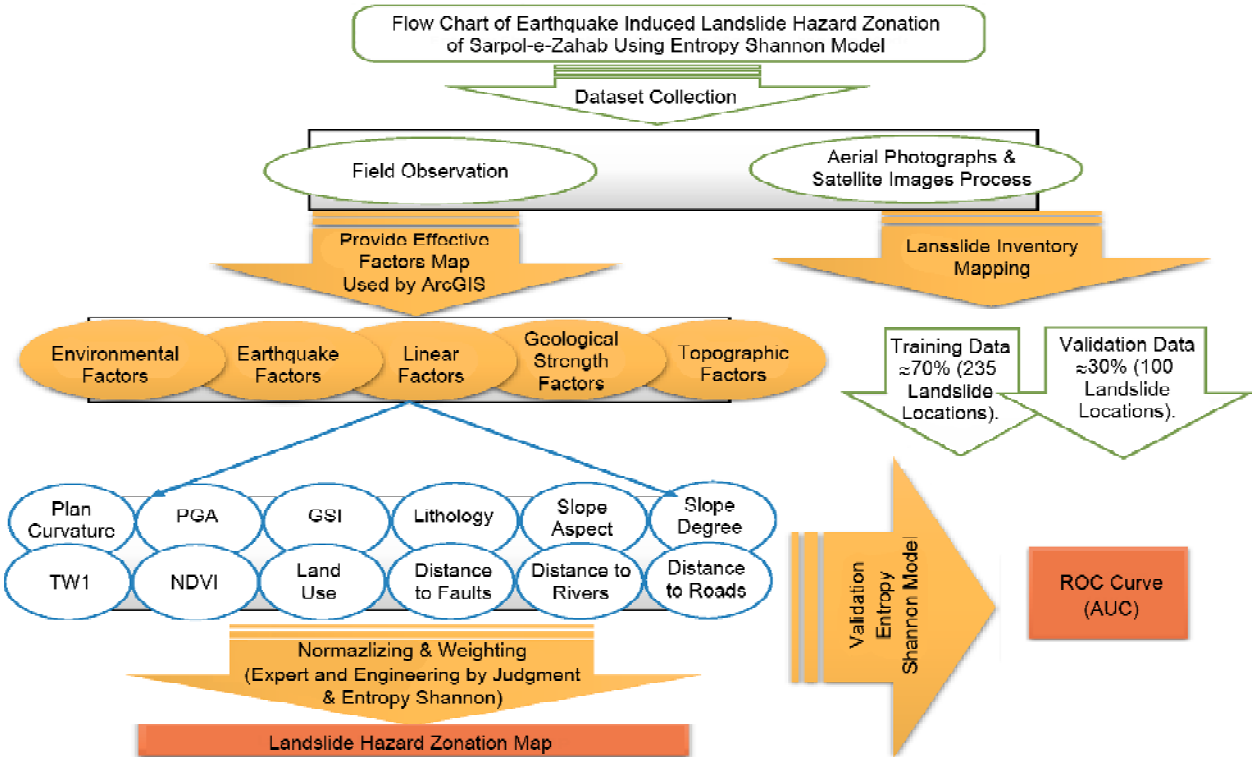

Figure 18. Flowchart of methodology and different research stages.

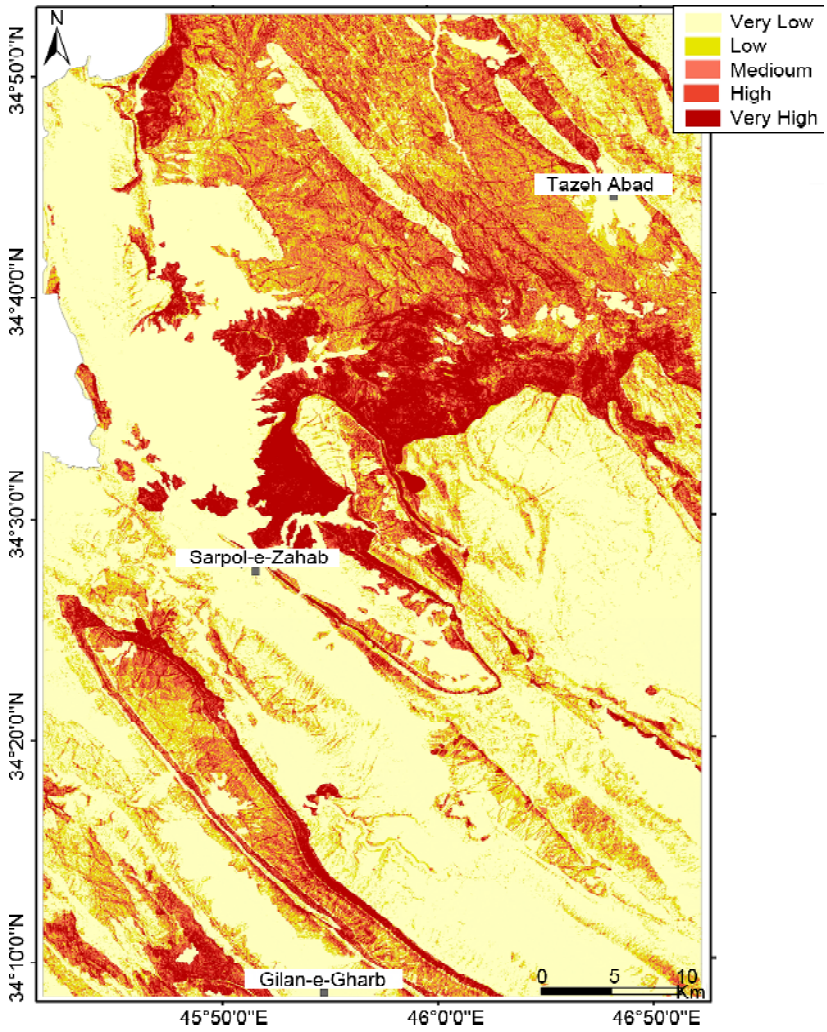

Figure 19. The Landslide Hazard Zonation map of Sarpol-e Zahab using Entropy Shannon Model.

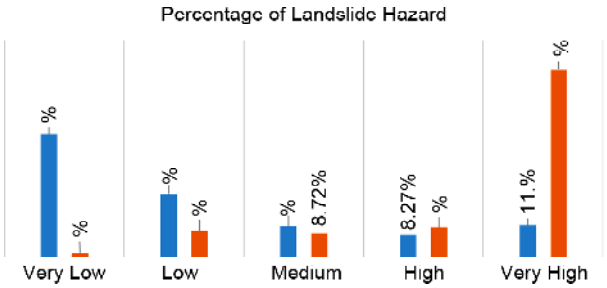

Figure 20. Column chart of the percentage of landslides in danger zones.

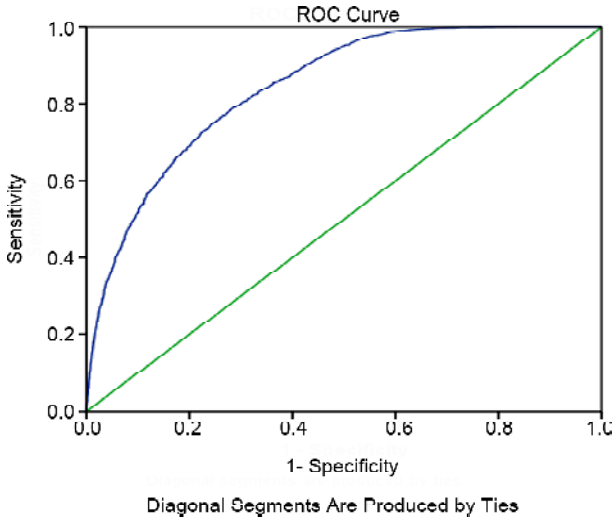

Figure 21. The ROC curve of Landslide Hazard Zonation map of Sarpol-e Zahab using Entropy Shannon model.

Table 3. Evaluation results (area under the curve) of Hazard Zonation map of Sarpol-e Zahab using Entropy Shannon model.

AUC	Std. Error	Asymptotic Sig	Asymptotic 95% Confidence Interval	
			Lower Bound	Upper Bound
0.843	0.002	0.000	0.839	0.848

The verification results showed that the index of the Entropy model (AUC = 84.3%) has high accuracy. The results of the ROC curve showed the accuracy of the mentioned model for the studied area is very good (Figure 21 and Table 3).

4. Results and Discussion

Landslides are considered one of the most dangerous natural disasters in the world. Much research has been done all over the world on the subject of landslide susceptibility, hazard and risk modeling. In this research, 12 effective factors were recognized that include Slope Angle, Slope Aspect, Lithology, Geological Strength Index (GSI), Distance to Faults, Peak Ground Acceleration (PGA), Plane Curvature, Distance to Roads, Distance to Rivers, Land Use, Normalized Difference Vegetation Index (NDVI) and topographic wetness index (TWI). The results of the implementation of Shannon's entropy model showed that the factors of Slope Angle (0.27), Lithology (0.22) and Geological Strength Index (0.22), are the most effective factors in the occurrence of landslides in the study area.

Finally, using the results of the entropy method, the effective factors were weighted. The final landslide hazard zonation map was prepared by the summation of weighted products of the effective parametric maps. After examining the importance of factors affecting the occurrence of landslides, the landslide hazard zoning map was prepared based on the relationships of the entropy model and divided into five classes as Very Low, Low, Medium, High and Very High. The area corresponding to each of the classes is 45.23, 23.40, 11.42, 8.27 and 11.67 percent, respectively. The area corresponding to each of the hazard classes was calculated as 11.67%, 8.27%, 11.42%, 23.40% and 45.23%, respectively. Also, the ratio of the areas involved in landslides to the hazard classes, from 68.94% (very high), 11.10% (high), 8.72% (medium), 9.65% (low) and 59.1% (very low), it was estimated that finally, the total areas involved in landslides occurred in the very high and high category, with more than 80% showing the high accuracy of the landslide hazard zonation map. The area corresponding to each of the hazard classes in the region was calculated as 11.67%, 8.27%, 11.42%, 23.40% and 45.23%, respectively.

Of the 335 landslides identified, 235 ($\approx$70%) locations were used for the landslide susceptibility maps, while the remaining 100 ($\approx$30%) cases were used for model validation. Finally, the ROC (receiver operating characteristic) curve for the landslide hazard zonation map was drawn and the areas under the curve (AUC) were calculated. The verification results showed that the index of the Entropy model (AUC = 84.3%) has high accuracy. The results of the ROC curve showed that the accuracy of the mentioned model for the studied area is very good. Considering the high accuracy of the presented model, the mentioned

landslide hazard zonation map can play a significant role in the planning and management of the region in order to prevent and reduce damages caused by landslides.

The results showed that in the future, the possibility of widespread slope instability will be very high and it is necessary to revise the land use plans of the region. Also, the possibility of this risk should be considered in the construction projects that are being built or will be built in the future, and measures to stabilize or avoid the risk should be considered in them. For example, observations showed that rural roads or access roads to many areas of forest and pasture lands have been built without observing any technical rules in the region, which in addition to increasing the risk of slope instability, it has created a high risk for the users of these roads. Also, some villages in the region (Mella Kabud and Qhorchi Bashi) are exposed to high risk in this regard, and appropriate solutions should be made with more detailed studies, such as relocation or adoption of stabilization and risk reduction methods in the region.

Acknowledgement

We would like to give special thanks to Mr. S. Mohammad Siavoshan from IIEES for his sincere comments and helps with editing the paper.

References

Alberti, S., Senogles, A., Kingen, K., Booth, A., Castro, P., DeKoekkoek, J., . . . Leshchinsky, B. (n.d.). The Hooskanaden Landslide: historic and recent surge behavior of an active earthflow on the Oregon Coast. *Landslides*, *17*, 2589-2602. doi:10.1007/s10346-020-01466-8

Aleotti, P., & Chowdhury, R. (1999). Landslide hazard assessment: summary review and new perspectives. *Bulletin Engineering Geology Environment*, *58*, 21-44.

Bednarik, M., Magulova, B., Matys, M., & Marschalko, M. (2010). Landslide susceptibility assessment of the Kralovany-Liptovsky Mikulas railway case study. *Physics and Chemistry of the Earth*, *35*(3), 162-171.

Coe, J.A. (2020). Bellwether sites for evaluating changes in landslide frequency and magnitude in cryospheric mountainous terrain: a call for systematic, long-term observations to decipher the impact of climate change. *Landslides*, *17*, 2483-2501. doi:10.1007/s10346-020-01462-y

Devkota, K.C., Regmi, A.D., Pourghasemi, H.R., Yoshida, K., Pradhan, B., Ryu, I.C., & Althuwaynee, O.F. (2013). Landslide susceptibility mapping using certainty factor, index of entropy and logistic regression models in GIS and their comparison at Mugling-Narayanghat road section in Nepal Himalaya. *Natural Hazards*, *65*(1), 135-165.

Dikshit, A., Raju, S., Biswajeet, P., Samuele, S., & Abdullah, M. A. (2020). Rainfall induced landslide studies in Indian Himalayan region: a critical review. *Applied Sciences*, *10*(7). doi:10.3390/app10072466

Froude, M.J., & Petley, D.N. (2018). Global fatal landslide occurrence from 2004 to 2016. Nat. *Hazards Earth Syst. Sci.*, *18*, 2161-2181. doi:10.5194/nhess-18-2161-2018

Galli, M., Ardizzone, F., Cardinali, M., Guzzetti, F., & Reichenbach, P. (2008). Comparing landslide inventory maps. *Geomorphology*, *94*, 268-289. doi:10.1016/j.geomorph.2006.09.023

Goetz, J., Guthriem, R., & Brenning, A. (2011). Integrating physical and empirical landslide susceptibility models using generalized additive models. *Geomorphology*, *129*, 367-386.

Guzzetti, F., Cardinali, M., Reichenbach, P., & Carrara, A. (2000). Comparing landslide maps: A case study in the Upper Tiber River Basin, central Italy. *Environ. Manag.*, *25*, 247-263.

Guzzetti, F., Mondini, A. C., Cardinali, M., Fiorucci, F., Santangelo, M., & Chang, K.-T. (2012). Landslide inventory maps: New tools for an old problem. *Earth-Sci. Rev.*, *112*, 42-66. doi:10.1016/j.earscirev.2012.02.001

Hao, L., Rajaneesh, A., Van Westen, C.,S., S.K., Martha, T.R., Jaiswal, P., & McAdoo, B.G. (2020). Constructing a complete landslide inventory dataset for the 2018 monsoon disaster in Kerala, India, for land use change analysis. E*arth Syst. Sci. Data*, 2899-2918. doi:10.5194/essd-12-2899-2020.

IAEG Commission on Landslides (1990). Suggested nomenclature for landslides. *Bulletin of the International Association of Engineering Geology*, 13-16. doi:10.1007/BF02590202.

IIEES (2017). *Earthquake report on November 11, 2017, Sarpol-e Zahab, Kermanshah province (5th Edition), Vol. I: Seismology (in Persian)*. International Institute Earthquake Engineering and Seismology.

IIEES (2017). *Earthquake report on November 11, 2017, Sarpol-e Zahab, Kermanshah province (5th edition), Vol. II: Geotechnical Phenomena (in Persian)*. International Institute Earthquake Engineering and Seismology.

ILWP. (2007). *Iranian Landslide Working Party, Iranian Landslides List*. Forest, Rangeland and Watershed Association.

Kanungo, D.A. (2006). A comparative study of conventional, ANN black box, fuzzy and combined neural and fuzzy weighting procedures for landslide susceptibility zonation in Darjeeling Himalayas. *Engineering Geology*, *85*, 347-366.

Karakas, G., Nefeslioglu, H., Kocaman, S., Buyukdemircioglu, M., Yurur, M., & Gokceoglu, C. (2021a). Derivation of earthquake-induced landslide distribution using aerial photogrammetry: the 24 January 2020 Elazig (Turkey) Earthquake. *Landslides*, *18*(2).

Kocaman, S., Tavus, B., Nefeslioglu, H.A., Karakas, G., & Gokceoglu, C. (2020). Evaluation of floods and landslides triggered by a meteorological catastrophe (Ordu, Turkey, August 2018) using optical and radar data. *Geofluids*, *12*, 1-18. doi: 10.1155/2020.

Lee, S., & Evangelista, D. (2006). Earthquake-induced landslide susceptibility mapping using an artificial neural network. Nat. *Hazards Earth Syst. Sci.*, *6*, 687-695. doi:10.5194/nhess-6-687-2006.

Li, X., Chen, Y., & Ouyang, H. (2002). Analysis on sand disaster with disaster entropy method. *Arid Land Geography*, *25*(4), 350-353.

Mateos, R.M., Lopez-Vinielles, J., Poyiadji, E., Tsagkas, D., Sheehy, M., Hadjicharalambous, K., ... Herrera, G. (2020). Integration of landslide hazard into urban planning across Europe. *Landscape Urban Plan*, *196*. doi:10.1016/j.landurbplan.2019.103740

Pourghasemi, H. R., Mohammady, M., & Pradhan, B. (2012). Landslide susceptibility mapping using index of entropy and conditional probability models in GIS: Safarood Basin, Iran. *Catena*, *97*, 71-84.

Rakhshandeh, M. (2018). *Developing Combined Solution for Landslide Hazard Zonation Using Neural-Fuzzy Network and Spatial Analysis*. M.Sc. Thesis. Tehran, Iran: Science and Research Branch, Islamic Azad University.

Regmi, A.D., Devkota, K.C., Yoshida, K., Pradhan, B., Pourghasemi, H. R., Kumamoto, T., & Akgun, A. (2014). Application of frequency ratio, statistical index, and weights-of-evidence models and their comparison in landslide susceptibility mapping in Central Nepal Himalaya. *Arabian Journal of Geosciences*, *7*(2), 725-742.

Rocscience Inc. (2007). RocLab Version 1.031- Rock mass strength analysis using the Hoek-Brown failure criterion.

Schuster, R. (1996). Socioeconomic Significance of Landslides. In A. Turner, & R. Schuster, *Landslides: Investigation and Mitigation, Transportation Research Board, Special Report*, 247 12-36. Washington, DC: National Academic Press.

Sevgen, E., Kocaman, S., Nefeslioglu, H.A., & Gokceoglu, C. (2019). A novel performance assessment approach using photogrammetric techniques for landslide susceptibility mapping with logistic regression, ANN and random forest. *Sensors*, *19*(18).

Sorensen, R., Zinko, U., & Seibert, J. (2006). On the calculation of the topographic wetness index: evaluation of different methods based on field observations. *Hydrology and Earth System Sciences Discussions*, *10*(1), 101-112.

Svennevig, K., Dahl-Jensen, T., Keiding, M., Merryman Boncori, J.P., Larsen, T.B., Salehi, S., . . . Voss, P. H. (2020a). Evolution of events before and after the 17 June 2017 rock avalanche at Karrat Fjord, West Greenland - a multidisciplinary

approach to detecting and locating unstable rock slopes in a remote Arctic area. *Earth Surf. Dynam.*, 1021-1038. doi:10.5194/esurf-8-1021-2020.

Tajik, V. (2009). *Landslide Hazard Zonation in Qeshm Island*. M.Sc. Thesis. Tehran, Iran: Science and Research Branch, Islamic Azad University.

Wang, Q., Li, W., Wu, Y., Pei, Y., & Xie, P. (2016). Application of statistical index and index of entropy methods to landslide susceptibility assessment in Gongliu (Xinjiang, China). *Environmental Earth Sciences*, *75*(5).

Yanar, T., Kocaman, S., & Gokceoglu, C. (2020). Use of Mamdani fuzzy algorithm for multi-hazard susceptibility assessment in a developing urban settlement (Mamak, Ankara, Turkey). *ISPRS International Journal of Geo-Information*, *9*(2). doi:10.3390/ijgi9020114

Yang, Z., & Qiao, J. (2009). Entropy-based hazard degree assessment for typical landslides in the three gorges area, China. *Environmental Science and Engineering*, 519-529.

Yang, Z., Qiao, J., & Zhang, X. (2010). Regional Landslide Zonation based on Entropy Method in Three Gorges Area, China. *Seventh International Conference on Fuzzy Systems and Knowledge Discovery (FSKD 2010)*, 1336-1339.

Yufeng, S., & Fengxiang, J. (2009). Landslide stability analysis based on generalized information entropy. *International Conference on Environmental Science and Information Application Technology*, (IEEE), *2*, 83-85.

Zinko, U., Seibert, J., Dynesius, M., & Nilsson, C. (2005). Plant species numbers predicted by a topography-based groundwater flow index. *Ecosystems*, *8*(4), 430-441.